

Simultaneous shape control and transport with multiple robots

Gonzalo López-Nicolás, Rafael Herguedas
Instituto de Investigación en Ingeniería de Aragón
Universidad de Zaragoza, Spain
gonlopez@unizar.es, rherguedas@unizar.es

Miguel Aranda, Youcef Mezouar
Université Clermont Auvergne, CNRS, SIGMA Clermont
Institut Pascal, F-63000 Clermont-Ferrand, France
first_name.last_name@sigma-clermont.fr

Abstract—Autonomous transport of objects may require multiple robots when the object is large or heavy. Besides, in the case of deformable objects, a set of robots may also be needed to maintain or adapt the shape of the object to the task requirements. The task we address consists in transporting an object, represented as a two dimensional shape or contour, along a desired path. Simultaneously, the team of robots grasping the object are controlled to the desired contour points configuration. Since the mobile robots of the team obey nonholonomic motion constraints, admissible trajectories are designed to keep the integrity of the object while following the prescribed path. Additionally, the simultaneous control of the object's shape is smoothly performed to respect the admissible deformation of the object. The main contribution lies in the definition of the grasping robots' trajectories dealing with the involved constraints. Different simulations, where the deformable object dynamics are modelled with consensus-based techniques, illustrate the performance of the approach.

I. INTRODUCTION

The robotic manipulation of deformable objects is a complex task that brings a number of challenges [1]: Model of the system, estimation of the states, controller design, kinematic and dynamic constraints, grasp configuration, etc. Additionally, several robots may be needed to perform the task depending on the object properties (e.g., size, weight, fragility, complex shapes). Although multirobot systems provide the ability to collectively carry out such complex tasks, they also pose new challenges [2].

Robotic manipulation of soft objects is still a complex and challenging problem of great interest. Possible applications span many areas such as surgery, food industry, manufacture of goods, or textile industry. In the context of medical applications, the task of deforming soft tissues into desired shapes has been addressed by means of an online estimation-recalibration algorithm to model local deformations [3]. The shape of the object was represented with Fourier series, and its physical properties were unknown. The control of elastic objects to achieve certain positions or shapes is also solved by using estimations of the Jacobian of the deformable

object [4]. The idea of *Indirect Simultaneous Positioning* [5] consists in controlling the position of points lying within the contour of a 2D deformable shape. The interest points are classified into grasping points and points which are controlled with a PID control. Another approach to control deformable objects whose model is unknown is based on learning their deformation parameters during visual-servo control and using these parameters for control predictions [6]. Certain objects, such as cables, can be considered as one-dimensional. The problem of deforming a cable with two manipulators has been solved by means of a local deformation model of the cable, which is based on Fourier series and estimated on-line [7]. Objects such as nets or fabrics can also be approximated by cables and modelled with the catenary curve equation [8]. Deformation tasks have also been studied using multirobot formation techniques [9].

Certain tasks require not only the control of the object's shape with multiple robots, but also its transport along a desired path. An example can be a sheet of a fragile material that needs to be transported through a narrow corridor or doorframe without compromising its integrity. Another example is a large piece of foam that needs to be transported and packed by deforming its shape to fit a box.

Transport of rigid and heavy objects with multiple mobile robots has already been studied [10], [11]. However, complexity greatly increases if the object is not rigid [12], [13], [14]. Autonomous transport of a deformable object has been performed with collaborative mobile manipulators [15], [16]. That task was solved with a two-level controller where the high-level control focuses on the motion planning and the low-level control handles collision avoidance and shape maintenance. In this paper, rather than shape maintenance, we focus on shape control while performing the transport task. An important challenge for these tasks is dealing with the motion constraints of the mobile platforms. For example, nonholonomic constraints were considered for a task of collaborative perception of a mobile target in [17].

In this paper, we consider the problem of simultaneously deforming and transporting a deformable object with multiple robots. The task is defined by a target shape for the object and a desired path to be followed. In this problem, we assume the position of each robot is known or can be estimated with a proper perception system. For a given set of grasping points,

This work was supported by the French Government through the RobotEx Equipment of Excellence (ANR-10-EQPX-44), the IMobS3 Laboratory of Excellence (ANR-10-LABX-16-01) and the I-SITE project CAP 20-25, and by the Spanish Government/European Union through project PGC2018-098719-B-I00 (MCIU/AEI/FEDER, UE), and project COMMANDIA SOE2/P1/F0638 (Interreg Sudoe Programme and European Regional Development Fund, ERDF).

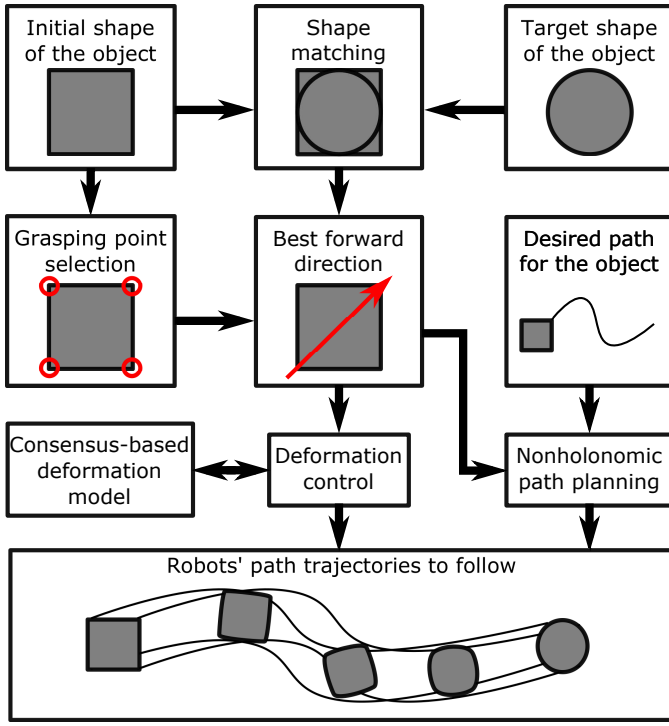


Fig. 1. Diagram of the main blocks of the proposal. The task is defined by the target shape of the object and the desired path to follow. The outputs are the appropriate trajectories for the grasp robots of the team.

we define the forward direction to move the team of robots with the object. Then, the main contribution is the definition of the admissible trajectories for each mobile robot grasping the object while taking into account the nonholonomic motion constraints of the platforms and the desired deformation process on the object.

The diagram in Fig. 1 presents the main blocks of the proposal. First, the initial and desired shapes of the object are matched (Section II-A). The procedure to compute the best direction to move forward and transport the object along the desired path is presented in Section II-B. The deformation control of the object (Section II-C) and path planning with nonholonomic motion constraints are jointly studied to define the trajectories that each robot has to follow (Section III). We consider isotropic and elastic materials and, in order to simulate the object deformation, we also propose a novel consensus-based model in Section IV. Several simulations in Section V test the proposal performance. Finally, conclusion is provided in Section VI.

II. SHAPE CONTROL OF THE OBJECT

Let us consider a two-dimensional shape defined by sampling the object's contour with M points $\mathbf{q}_j \in \mathbb{R}^2$ expressed in a global reference frame in their centroid:

$$\mathbf{q}(t) = \{\mathbf{q}_j(t) = (q_{xj}, q_{yj})^T, j = 1, \dots, M\}, \quad (1)$$

where \mathbf{q}_j are stacked in matrix form as $\mathbf{q} \in \mathbb{R}^{2 \times M}$. Similarly, let us define the desired final shape of the object with the set

of target contour points $\mathbf{c}_j \in \mathbb{R}^2$ with $\mathbf{c} \in \mathbb{R}^{2 \times M}$ expressed in a global reference frame in their centroid:

$$\mathbf{c} = \{\mathbf{c}_j = (c_{xj}, c_{yj})^T, j = 1, \dots, M\}. \quad (2)$$

A. Initial and target shape matching

In order to perform adequately the shape control, we need first to match each of the contour grasping points of the initial shape with a corresponding point on the target shape. This matching can be effectively performed by taking advantage of the orthogonal Procrustes shape-alignment problem [18].

In particular, let us consider the two sets of points are the initial shape \mathbf{q} defined by each of the discretized contour points of the object \mathbf{q}_j and the desired shape \mathbf{c} defined by contour points \mathbf{c}_j . We evaluate M different sets of correspondences by matching \mathbf{q}_1 with each \mathbf{c}_j . In each set, the rest of correspondences directly follows since the order of the sequence of points is fixed, i.e. $\{(\mathbf{q}_1, \mathbf{c}_j), (\mathbf{q}_2, \mathbf{c}_{j+1}), (\mathbf{q}_3, \mathbf{c}_{j+2}), \dots\}$. For each set of correspondences, the shape-alignment problem is solved by computing the rotation matrix $\mathbf{R} \in \mathcal{SO}(2)$ that minimizes the dissimilarity between \mathbf{q} and \mathbf{c} by solving $\arg \min_{\mathbf{R}} \|\mathbf{q} - \mathbf{R}\mathbf{c}\|_F$ with F denoting the Frobenius norm. Finally, the set of correspondences that provide the minimum residue is selected. Note that more sophisticated approaches can be found, for instance by explaining deformations of the prescribed shape by means of elastic forces acting on the shape boundary and minimizing the area of mutual non-overlap [19]. Figure. 2 shows examples of current and desired object shape.

B. Selection of forward direction of motion

Once the object is grasped, the direction of translation needs to be defined. Since the mobile robots transporting the object obey nonholonomic motion constraints, the direction to carry out the forward motion should be properly selected. In general, this decision can be inherently provided by the particular task. For instance, for traversing a narrow corridor with an elongated shaped object, it would be appropriate to translate along the larger dimension of the object. However, if there is no particular prescribed direction of motion, we can seek the best direction of motion in order to minimize the individual motion of the mobile grasp robots by taking into account the specified deformation. We describe how to do this next.

The grippers for shape control or cooperative transport tasks are usually considered as point robots firmly attached to the deformable object [8], [13], [20]. Similarly, we consider that each grasping point consists of a mobile robot, with unicycle kinematics, mounting a robotic tool able to firmly grasp the object imposing the translational degrees of freedom of each grasp with free orientation. This robotic tool could be a manipulator arm, or just a rotary gripper on the mobile platform as proposed here. Considering M grasping points, we compute the error matrix $\mathbf{e} \in \mathbb{R}^{2 \times M}$ defined as the difference of the matched contour points between the initial \mathbf{q} and target \mathbf{c} shapes:

$$\mathbf{e} = \mathbf{q} - \mathbf{R}\mathbf{c}. \quad (3)$$

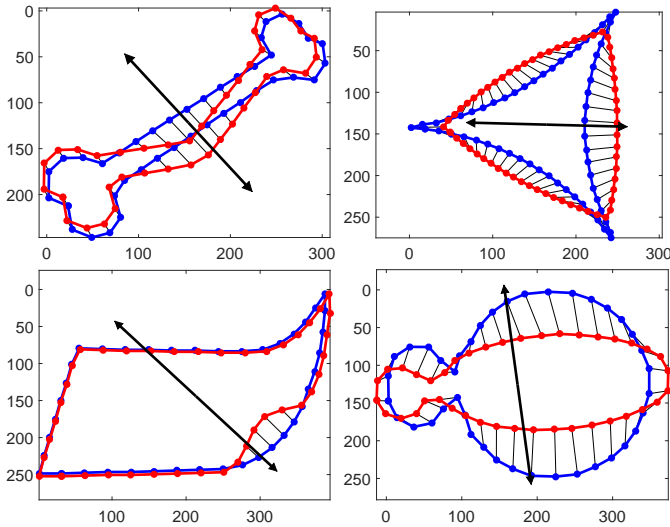


Fig. 2. Examples with the selected orientation to define the forward motion direction for the object translation. Both the initial and target shapes are drawn, respectively, in blue and red colours. The grasping points are plotted with dots, and these dots are linked with thin straight lines showing the desired deformation. The black arrow represents the computed orientation α .

We propose the computation of the object direction of motion by means of Principal Component Analysis (PCA). Thus, we subtract the mean for each dimension $\bar{\mathbf{e}} = \mathbf{e} - \frac{1}{M} \mathbf{e} \mathbf{1}_{M \times M}$ on the error components. Then, the singular value decomposition $\bar{\mathbf{e}} = \mathbf{U} \mathbf{S} \mathbf{V}^T$ gives the matrix \mathbf{V} that contains the eigenvectors of $\bar{\mathbf{e}} \bar{\mathbf{e}}^T$ and the columns of \mathbf{V} are the principal components of \mathbf{e} . Finally, the best orientation to perform the translation of the object, in terms of minimizing the path followed by the robots for the deformation process, is given by $\alpha = \text{atan2}(V_{2,1}, V_{1,1})$ with $V_{n,m}$ the element of n -row and m -column of \mathbf{V} , and $\text{atan2}: \mathbb{R}^2 \rightarrow (-\pi, \pi]$ is a four-quadrant arctangent function. Figure 2 displays several examples where the selection of the orientation α follows the proposed method.

C. Shape control

Let us consider N mobile robots and the corresponding N grasping points to control the shape of an object. Choosing a good grasp configuration is a complex task that involves evaluation of quality measures [21]. Here, the grasping points are selected beforehand within the set of contour sampled points of the object \mathbf{q}_j such that $N \leq M$. Adequate grasping points selection will heavily depend on the complexity of the object shape but, in general, an equally spaced distribution around the contour shape will suffice. Here, we assume the robots are initially positioned in their corresponding selected grasping points. The robots' states in a fixed global reference frame are given by $\mathbf{x}_i(t) = (x_i(t), y_i(t))^T$ and $\phi_i(t)$, with $i = 1, \dots, N$. The robots obey unicycle kinematics

$$\dot{x}_i = v_i \cos \phi_i, \quad \dot{y}_i = v_i \sin \phi_i, \quad \dot{\phi}_i = \omega_i, \quad (4)$$

with $v_i(t)$ and $\omega_i(t)$ being the linear and angular velocities. The position of the robots in the current grasping points set \mathbf{q}_i , and the desired shape points \mathbf{c}_i , can be expressed in polar

coordinates as

$$\begin{aligned} \rho_{qi} &= \sqrt{q_{xi}^2 + q_{yi}^2}, & \theta_{qi} &= \text{atan2}(q_{yi}, q_{xi}) \\ \rho_{ci} &= \sqrt{c_{xi}^2 + c_{yi}^2}, & \theta_{ci} &= \text{atan2}(c_{yi}, c_{xi}) \end{aligned} \quad (5)$$

Now, we impose an exponential evolution to the grasping points on the object's contour from the initial configuration $(\rho_{qi}(t=0), \theta_{qi}(t=0))$ to the desired one (ρ_{ci}, θ_{ci}) , i.e.,

$$\begin{aligned} \dot{\rho}_{qi} &= -k_\rho (\rho_{qi} - \rho_{ci}) \\ \dot{\theta}_{qi} &= -k_\theta (\theta_{qi} - \theta_{ci}) \end{aligned} \quad (6)$$

being k_ρ and k_θ positive control gains. Therefore,

$$\begin{aligned} \rho_{qi} &= \rho_{ci} + (\rho_{qi}(t=0) - \rho_{ci}) \exp(-k_\rho t) \\ \theta_{qi} &= \theta_{ci} + (\theta_{qi}(t=0) - \theta_{ci}) \exp(-k_\theta t) \end{aligned} \quad (7)$$

III. PATH PLANNING FOR GRASP ROBOTS

Simultaneously to the object deformation, the centroid of the object is also required to follow a desired path defined by a virtual robot with position $\mathbf{x}_t(t) = (x_t(t), y_t(t))^T$ and orientation $\phi_t(t)$. We assume that the motion of the virtual robot is defined with its linear and angular velocities, $v_t(t)$ and $\omega_t(t)$, and that the produced trajectory along the desired path obeys unicycle kinematics

$$\dot{x}_t = v_t \cos \phi_t, \quad \dot{y}_t = v_t \sin \phi_t, \quad \dot{\phi}_t = \omega_t. \quad (8)$$

The choice of this constraint on the desired path implies that such path can be followed by mobile platforms with unicycle kinematics.

A. Reference trajectories design

Taking into account the desired deformation control process (Section II-C) and the desired path to be followed (8), the trajectories to be tracked by each of the grasp robots are defined in the following. The reference trajectory for robot i is denoted with $\mathbf{x}_{ri}(t) = (x_{ri}(t), y_{ri}(t))^T$ and orientation $\phi_{ri}(t)$, with $i = 1, \dots, N$. In order to create feasible trajectories we impose unicycle kinematics

$$\dot{x}_{ri} = v_{ri} \cos \phi_{ri}, \quad \dot{y}_{ri} = v_{ri} \sin \phi_{ri}, \quad \dot{\phi}_{ri} = \omega_{ri}, \quad (9)$$

where $v_{ri}(t)$ and $\omega_{ri}(t)$ are the linear and angular velocities that generate the reference trajectories to be tracked by the grasp robots.

Given the target path to be followed (x_t, y_t, ϕ_t) or, alternatively, the velocities v_t and ω_t , we express the coordinates of each robot (4) with respect to the target path:

$$\mathbf{x}_{ri} = \mathbf{R}(\phi_t) \mathbf{q}_i + \mathbf{x}_t, \quad (10)$$

where $\mathbf{R}(\phi_t) \in \mathcal{SO}(2)$ is a rotation matrix

$$\mathbf{R}(\phi_t) = \begin{bmatrix} \cos(\phi_t) & -\sin(\phi_t) \\ \sin(\phi_t) & \cos(\phi_t) \end{bmatrix}. \quad (11)$$

Using polar coordinates (5), (10) reduces to

$$\mathbf{x}_{ri} = \rho_{qi} \begin{pmatrix} \cos(\phi_t + \theta_{qi}) \\ \sin(\phi_t + \theta_{qi}) \end{pmatrix} + \mathbf{x}_t, \quad (12)$$

Calculating the time derivative of this vector yields

$$\dot{\mathbf{x}}_{ri} = \frac{\partial \mathbf{R}(\phi_t + \theta_{qi})}{\partial (\phi_t + \theta_{qi})} \begin{pmatrix} \rho_{qi} (\omega_t + \dot{\theta}_{qi}) \\ -\dot{\rho}_{qi} \end{pmatrix} + \dot{\mathbf{x}}_t. \quad (13)$$

with $\dot{\mathbf{x}}_t$ in (8), $\dot{\rho}_{qi}$, $\dot{\theta}_{qi}$ defined in (6) and

$$\frac{\partial \mathbf{R}(\phi_t + \theta_{qi})}{\partial (\phi_t + \theta_{qi})} = \begin{bmatrix} -\sin(\phi_t + \theta_{qi}) & -\cos(\phi_t + \theta_{qi}) \\ \cos(\phi_t + \theta_{qi}) & -\sin(\phi_t + \theta_{qi}) \end{bmatrix}. \quad (14)$$

The reference orientation ϕ_{ri} is then obtained as $\phi_{ri} = \arctan(\dot{y}_{ri} / \dot{x}_{ri})$, with $\phi_{ri}(t=0) = \phi_t(t=0)$. Finally, the reference velocities for the robots are computed with

$$v_{ri} = \sqrt{x_{ri}^2 + y_{ri}^2} \quad (15)$$

$$\omega_{ri} = \dot{\phi}_{ri} = \frac{d}{dt} \arctan \frac{\dot{y}_{ri}}{\dot{x}_{ri}}. \quad (16)$$

B. Tracking control

In order to perform the tracking of the reference trajectories produced by v_{ri} and ω_{ri} (15)-(16) we define the tracking error in position $\mathbf{x}_{ei}(t) = (x_{ei}(t), y_{ei}(t))^T$ and orientation $\phi_{ei}(t)$, with $i = 1, \dots, N$,

$$\mathbf{x}_{ei} = (\mathbf{R}(\phi_{ri}))^T (\mathbf{x}_i - \mathbf{x}_{ri}) \quad (17)$$

$$\phi_{ei} = \phi_i - \phi_{ri}, \quad (18)$$

Next, we compute the grasp robots velocities based on the tracking control law presented by Morin and Samson [22](chapter 34):

$$v_i = \frac{1}{\cos \phi_{ei}} (v_{ri} - k_r |v_{ri}| (x_{ei} + y_{ei} \tan \phi_{ei})), \quad (19)$$

$$\omega_i = \omega_{ri} - (k_y v_{ri} y_{ei} + k_\phi |v_{ri}| \tan \phi_{ei}) \cos^2 \phi_{ei}, \quad (20)$$

being k_r , k_y , and k_ϕ positive control gains. Notice that, for this tracking to be feasible, the following assumption is required:

Assumption 1: The velocities v_t and ω_t are bounded differentiable functions with bounded derivative, and v_t does not tend to zero over time until the end of the desired path.

C. Stability Analysis of the tracking control

The stability of the tracking control (19)-(20) can be analyzed through the Lyapunov function [22](chapter 34)

$$V = \sum_{i=1}^N V_i \quad (21)$$

with

$$V_i = \frac{1}{2} \left(\mathbf{x}_{ei}^T \mathbf{x}_{ei} + \frac{1}{k_y} \tan^2 \phi_{ei} \right). \quad (22)$$

The derivative of V_i is

$$\dot{V}_i = \mathbf{x}_{ei}^T \dot{\mathbf{x}}_{ei} + \frac{\dot{\phi}_{ei} \tan \phi_{ei}}{k_y \cos^2 \phi_{ei}}. \quad (23)$$

Working out the i term of the Lyapunov function with (17), (18), and (20), yields

$$\begin{aligned} \dot{V}_i &= (\mathbf{x}_i - \mathbf{x}_{ri})^T (\dot{\mathbf{x}}_i - \dot{\mathbf{x}}_{ri}) + \frac{\dot{\phi}_{ei} \tan \phi_{ei}}{k_y \cos^2 \phi_{ei}} \\ &= \mathbf{x}_{ei}^T (\mathbf{R}(\phi_{ri}))^T (\dot{\mathbf{x}}_i - \dot{\mathbf{x}}_{ri}) \\ &\quad - v_{ri} y_{ei} \tan \phi_{ei} - \frac{k_\phi}{k_y} |v_{ri}| \tan^2 \phi_{ei}. \end{aligned} \quad (24)$$

Finally, using (11), (4), and (9) with (19) in (24) we have

$$\begin{aligned} \dot{V}_i &= -k_r |v_{ri}| (x_{ei} + y_{ei} \tan \phi_{ei})^2 \\ &\quad - \frac{k_\phi}{k_y} |v_{ri}| \tan^2 \phi_{ei}. \end{aligned} \quad (25)$$

Therefore, since $\dot{V}_i \leq 0$, \dot{V} is negative semi-definite. In this system, the evolution with time of v_{ri} is bounded with bounded derivative (as a consequence of (12) and (15) with Assumption 1). Then, using Barbalat's lemma [23], we have $\dot{V} \rightarrow 0$ when $t \rightarrow \infty$ and, since v_{ri} does not tend to zero (Assumption 1), we have $\phi_{ei} = 0$ and $x_{ei} = 0$. Besides, since $\phi_{ei} = \omega_i - \omega_{ri}$ and from (20) we have $y_{ei} = 0$. Therefore, the tracking control is globally asymptotically stable.

IV. CONSENSUS-BASED DEFORMATION MODEL

One of the simplest approaches to simulate deformable objects is the mass-spring model. For example, discrete networks of mass-spring-damper elements are used to model a deformable object controlled from the initial to the final shape by manipulators [20]. Mass-spring-based models are generally not accurate for large deformations and flips of the mesh can be produced during deformations. A classical alternative to model elastic objects is the Finite Element Method (FEM) [24]. Nevertheless, FEM models are computationally expensive and usually require a great effort in defining the initial parameters of the system and are sensitive to the mesh discretization. Opposed to these methods, the Meshless Shape Matching (MSM) approach provides advantages such as controllability and computational efficiency. In particular, recent approaches are able to learn the deformability object properties without performing force measurements using MSM methods [25].

Next, we present a simple and novel deformation model based on consensus techniques [26] [27]. The proposed model is intended for isotropic and elastic materials assumed to be initially at rest. The main idea is that some points of the object will be grasped and moved away from the equilibrium state and the rest of the object, represented by a mesh of nodes, will evolve following a consensus based algorithm. Thus, we model the matter interaction with a communication graph between nodes and the tuned properties of a consensus algorithm. A main advantage of this approach is the possibility of taking advantage of the well-established formalization techniques in the field of consensus algorithms. The validity of this model is illustrated in Section V where some simulations show good visual performance of the object deformation.

Consider the object of interest defined by a set of nodes $\mathbf{x}_n \in \mathbb{R}^{2 \times P}$ evenly distributed over the shape surface where

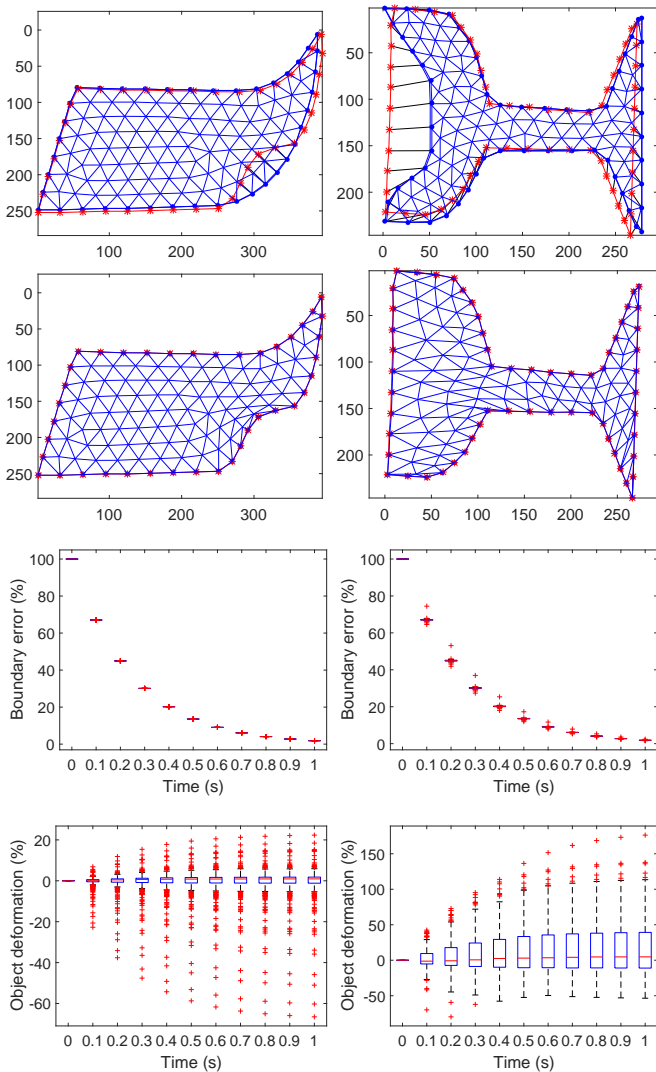


Fig. 3. Each column shows a different example of object deformation. From top to bottom: Initial shape with the desired contour shape; Final shape after the deformation control; Evolution over time of the contour shape error; Evolution of the object deformation over time measured with the arc lengths of the object mesh.

each node has coordinates $\mathbf{x}_{np} = (\mathbf{x}_{n xp}, \mathbf{x}_{n yp})^T$, with $p = 1, \dots, P$. Note that this set of points includes the contour points $\mathbf{q} \in \mathbb{R}^{2 \times M}$. A set of points \mathbf{q}_i with $i = 1, \dots, N$ of the contour is selected as grasping points to actuate on the object. A triangular mesh is also defined between the nodes \mathbf{x}_n . Then, the system can be represented by an undirected graph $\mathcal{G} = (\mathcal{V}, \mathcal{E})$, where $\mathcal{V} = 1, \dots, P$ is the node set and $\mathcal{E} \subseteq \mathcal{V} \times \mathcal{V}$ is the edge set, where the edges are those of the triangular mesh. The Laplacian matrix of \mathcal{G} is $\mathbf{L} = \mathbf{D} - \mathbf{A}$ where \mathbf{D} is the degree matrix and \mathbf{A} is the adjacency matrix of the graph.

At each sampling instant k (so $t = kT$ with T the sampling time), we compute the imposed deformation of the grasp contour points from (7):

$$\mathbf{q}_i(k) = \begin{pmatrix} \rho_{q_i}(k) \cos \theta_{q_i}(k) \\ \rho_{q_i}(k) \sin \theta_{q_i}(k) \end{pmatrix}, \text{ with } i = 1, \dots, N. \quad (26)$$

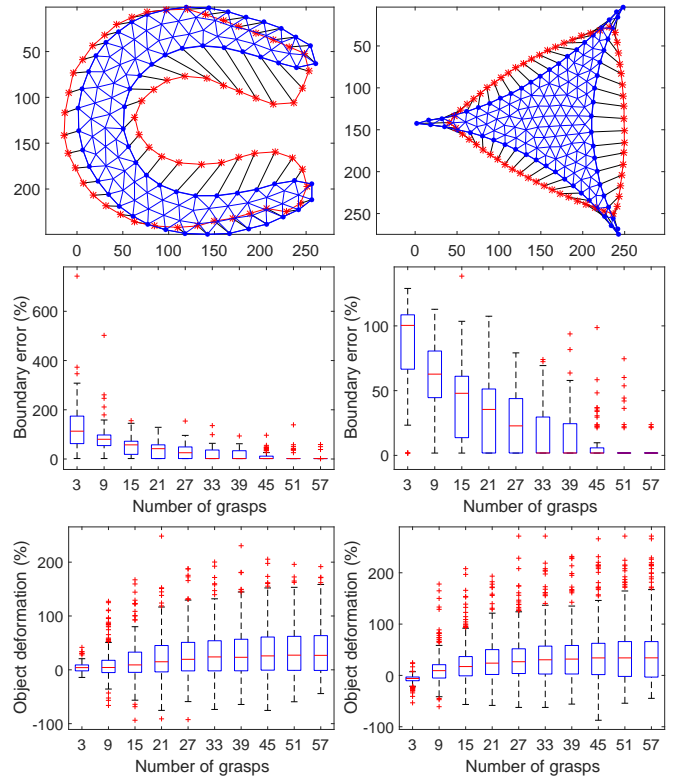


Fig. 4. Each column shows a different example. From top to bottom: Initial shape with the desired contour shape; Final contour shape error as a function of the number of object grasps; Final object deformation as a function of the number of object grasps.

We define $\tilde{\mathbf{x}}_n$ as \mathbf{x}_n updating the values of the contour grasping points with $\mathbf{q}_i(k)$ from (26). The consensus algorithm is then executed $m = \text{floor}(T/\delta)$ times (with floor the round function towards minus infinity),

$$\mathbf{x}_n(m+1) = \tilde{\mathbf{x}}_n(m) - \delta K \mathbf{L} (\tilde{\mathbf{x}}_n(m) - \mathbf{x}_n(m)), \quad (27)$$

where the time step is δ and K is a positive gain. The consensus algorithm is initialized each kT with $\tilde{\mathbf{x}}_n(m=0) = \tilde{\mathbf{x}}_n(k)$ and $\mathbf{x}_n(m=0) = \mathbf{x}_n(k)$. Then, the evolution of the object deformation is given by the state of the nodes computed at every sampling instant k with the consensus algorithm (27). Properties of the deformable object, such as elasticity or plasticity, can be modelled by tuning the consensus parameters (δ, K) , but comprehensive analysis is left for future work.

V. SIMULATIONS

The following simulations illustrate the performance of the proposal. Some basic shapes are expressly defined for some of the examples, and the rest are selected from dataset MPEG-7 [28]. The first examples show the control of the object deformation from the initial to the desired contour shape (Fig. 3). In this case, the number of grasping points is selected as $N = M$. The evolution of the boundary error ϵ presents the expected behaviour as the object is deformed. This error is defined as follows

$$\epsilon_j = 100 \frac{\|\mathbf{c}_j - \mathbf{q}_j(t)\|}{\|\mathbf{c}_j - \mathbf{q}_j(t=0)\|}, \quad j = \{1, \dots, M\}. \quad (28)$$

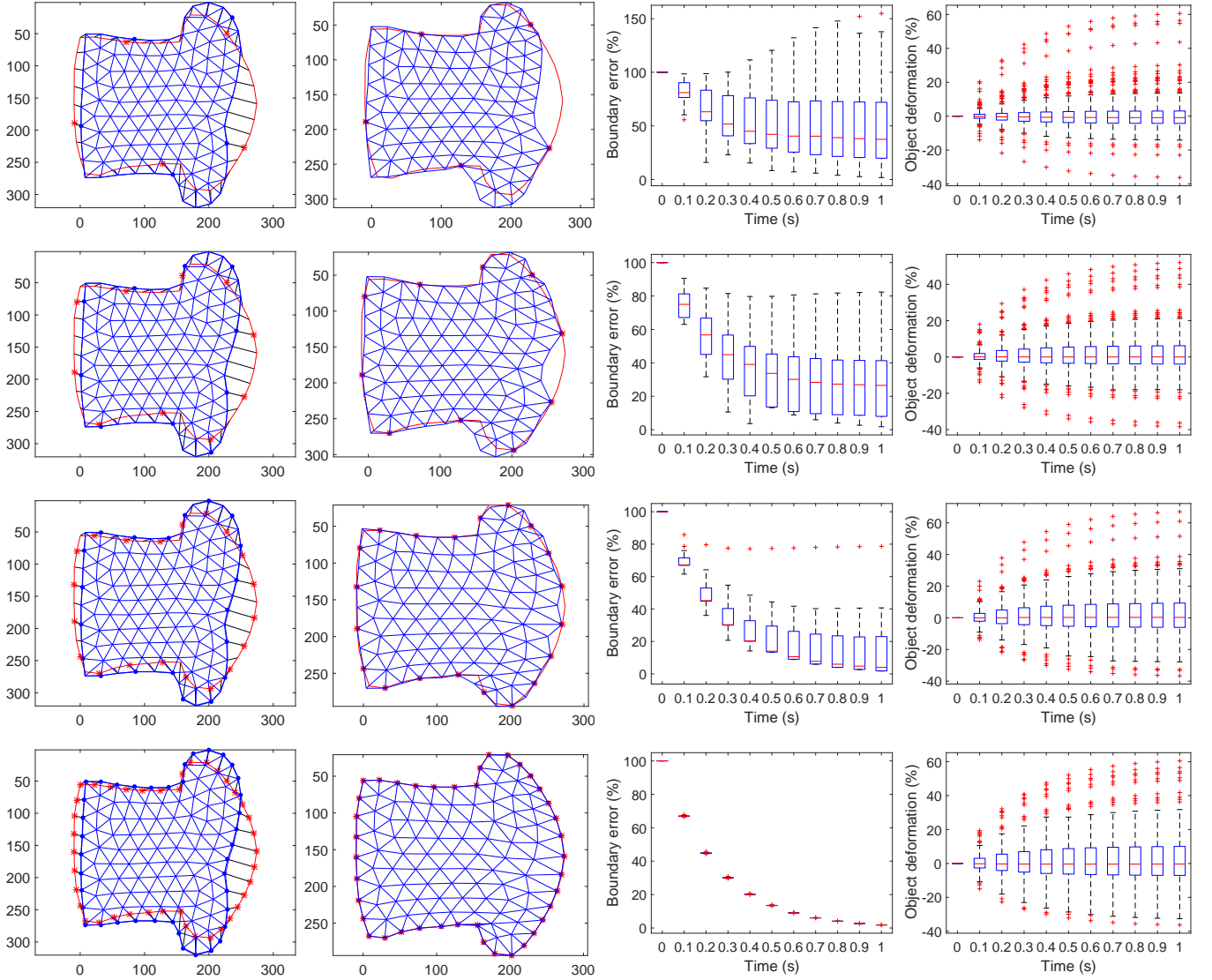


Fig. 5. Example of object deformation where the number of grasping points is different in each row of the figure: $N = \{5, 10, 20, 40\}$. From left to right: Initial shape with the desired contour shape and the selected grasping points marked with asterisks; Final shape after the deformation control; Evolution over time of the contour shape error; Evolution of the object deformation over time.

being \mathbf{q}_j and \mathbf{c}_j the M boundary points as defined in (1) and (2). The plot of the object deformation presents statistical results on how the object is stretched or compressed by measuring the length of the arcs in the triangular mesh. In particular, we define the object deformation (stretch or compression) as follows

$$\sigma_{rs} = 100 \left(\frac{\|\mathbf{x}_{nr}(t) - \mathbf{x}_{ns}(t)\|}{\|\mathbf{q}_{nr}(t=0) - \mathbf{q}_{ns}(t=0)\|} - 1 \right), \quad (29)$$

where $r \neq s$ with $r, s \in \{1, \dots, P\}$ and $\forall(r, s) \in \mathcal{E}$. In the first example of Fig. 3 only a small part of the object is compressed as seen in the deformation plot. In the second example, the object deformation is more distributed.

The tests in Fig. 4 are similar to the ones of the previous case, but now the number of grasping points is modified to show the variation in the results. Different simulations

are carried out with different number of grasps. Namely, $N = \{3, 9, 15, 21, 27, 33, 39, 45, 51, 57\}$. For each case, the grasping points are evenly distributed around the object boundary. As the number of grasping points increases, the final error decreases, and the object deformation increases since the action is performed in more object points. In these previous tests, the final result after each execution is depicted. The example in Fig. 5 also focuses on the effect of the number of grasps showing the results evolving over time for a particular shape. The results show that increasing the number of grasps results in less dispersion on the deformation error and more homogeneous deformation.

The proposed method for object deformation and transport is illustrated in Fig. 6. The examples show the motion of the object following the target path (an eight-shape depicted with thick red line) while performing the desired object

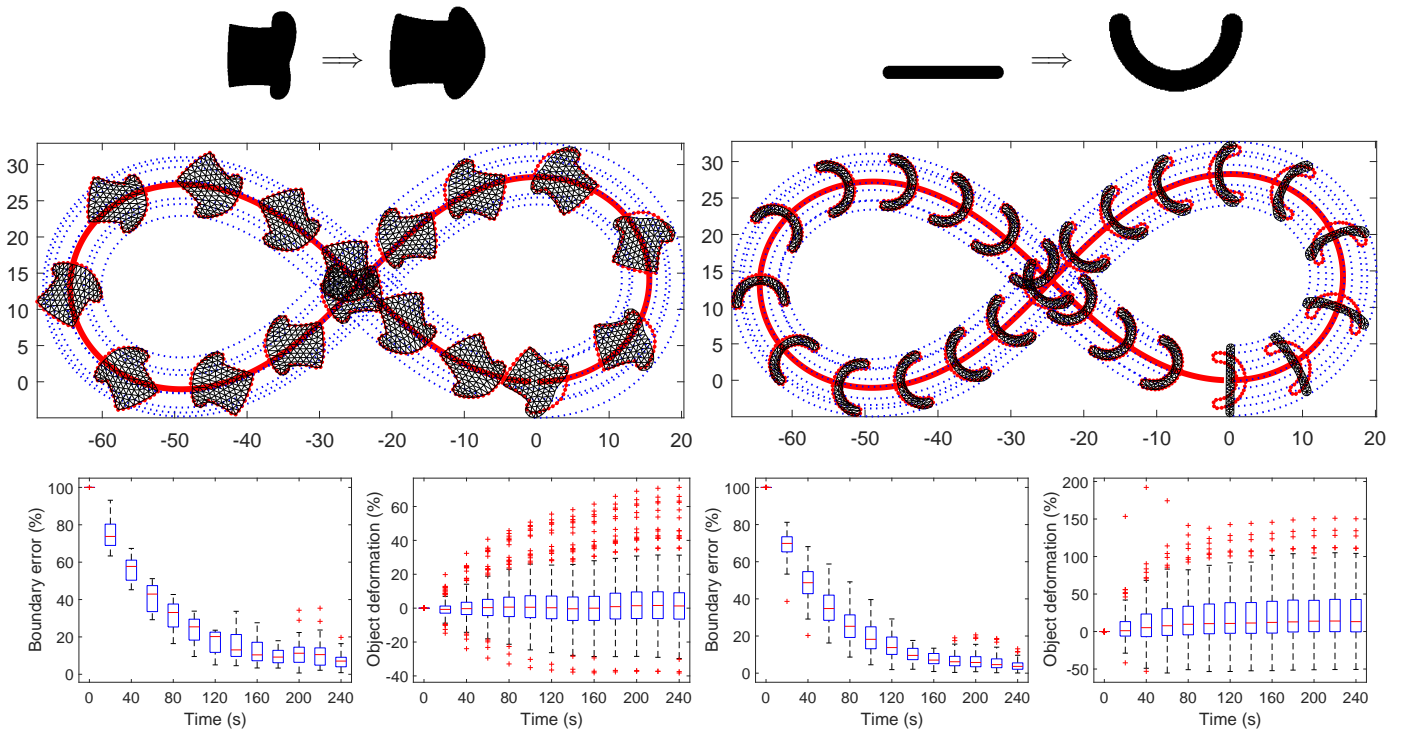


Fig. 6. Two different examples of object deformation and transport following an eight-shape trajectory. Black icons on top show the initial and desired object deformation. Plots on the second row depict the path followed by the grasping points while performing the object deformation with starting position at (0,0); Third row shows the evolution over time of the contour shape error; and the evolution of the object deformation during the transport and shape control.

deformation. In these simulations the tracking control is not evaluated, and perfect data measurements is assumed as well as perfect robot control. The first example is the shape of a hat performing some deformation and the second one is an I-shape deformed to a C-shape.

A video attachment is provided to show several examples of the approach¹. It also includes an illustrative case where the object is deformed to pass through a narrow corridor and it subsequently recovers its initial shape.

VI. CONCLUSIONS

In this paper, the task of transporting an object while simultaneously performing shape control is addressed. We design appropriate trajectories that take into account both the nonholonomic motion constraints of the robots grasping the object and the smooth deformation requirements. The proposed trajectories for the grasp robots are successfully followed with a tracking control law, while the proposed model of the deformable object to evaluate the proposal with consensus-based techniques shows good performance. Our proposal brings several aspects worth to further investigate. Future work may include the study of an automatic procedure to select adequate number of grasps and their location on the object. Another open issue is to investigate procedures to check the feasibility or reachability of a particular deformation. The study of the properties of the consensus-based deformation model is also a promising research line. For example, it is

worth to investigate if the deformation model can be used for prediction during the control.

REFERENCES

- [1] J. Sanchez, J. A. Corrales, B. C. Bouzgarrou, and Y. Mezouar, "Robotic manipulation and sensing of deformable objects in domestic and industrial applications: a survey," *The International Journal of Robotics Research*, vol. 37, no. 7, pp. 688–716, 2018.
- [2] K.-K. Oh, M.-C. Park, and H.-S. Ahn, "A survey of multi-agent formation control," *Automatica*, vol. 53, pp. 424–440, 2015.
- [3] D. Navarro-Alarcon and Y. H. Liu, "Fourier-based shape servoing: a new feedback method to actively deform soft objects into desired 2-D image contours," *IEEE Transactions on Robotics*, vol. 34, no. 1, pp. 272–279, 2018.
- [4] D. Navarro-Alarcon, H. M. Yip, Z. Wang, Y. H. Liu, F. Zhong, T. Zhang, and P. Li, "Automatic 3-D manipulation of soft objects by robotic arms with an adaptive deformation model," *IEEE Transactions on Robotics*, vol. 32, no. 2, pp. 429–441, 2016.
- [5] T. Wada, S. Hirai, S. Kawamura, and N. Kamiji, "Robust manipulation of deformable objects by a simple PID feedback," in *IEEE International Conference on Robotics and Automation (ICRA)*, May 2001, pp. 85–90.
- [6] Z. Hu, P. Sun, and J. Pan, "Three-dimensional deformable object manipulation using fast online gaussian process regression," *IEEE Robotics and Automation Letters*, vol. 3, no. 2, pp. 979–986, 2018.
- [7] J. Zhu, B. Navarro, P. Fraitse, A. Crosnier, and A. Cherubini, "Dual-arm robotic manipulation of flexible cables," in *IEEE/RSJ International Conference on Intelligent Robots and Systems (IROS)*, Nov. 2018, pp. 479–484.
- [8] R. Cotsakis, D. St-Onge, and G. Beltrame, "Decentralized collaborative transport of fabrics using micro-UAVs," in *IEEE International Conference on Robotics and Automation (ICRA)*, May 2019, pp. 7734–7740.
- [9] M. Aranda, J. A. Corrales, and Y. Mezouar, "Deformation-based shape control with a multirobot system," in *IEEE International Conference on Robotics and Automation (ICRA)*, 2019, pp. 2174–2180.
- [10] D. Rus, B. Donald, and J. Jennings, "Moving furniture with teams of autonomous robots," in *IEEE/RSJ International Conference on Intelligent Robots and Systems (IROS)*, vol. 1, Aug. 1995, pp. 235–242.

¹<http://webdiis.unizar.es/%7Eglopez/videos.html>

- [11] Z. Wang and M. Schwager, "Kinematic multi-robot manipulation with no communication using force feedback," in *IEEE International Conference on Robotics and Automation (ICRA)*, Jun. 2016, pp. 427–432.
- [12] D. Sun, J. K. Mills, and Y.-H. Liu, "Position control of robot manipulators manipulating a flexible payload," *The International Journal of Robotics Research*, vol. 18, no. 1995, pp. 319–332, 1999.
- [13] H. Bai and J. T. Wen, "Cooperative load transport: a formation-control perspective," *IEEE Transactions on Robotics*, vol. 26, no. 4, pp. 742–750, 2010.
- [14] R. Herguedas, G. López-Nicolás, R. Aragüés, and C. Sagüés, "Survey on multi-robot manipulation of deformable objects," in *24th IEEE International Conference on Emerging Technologies and Factory Automation (ETFA)*, 2019, pp. 977–984.
- [15] J. Alonso-Mora, R. Knepper, R. Siegwart, and D. Rus, "Local motion planning for collaborative multi-robot manipulation of deformable objects," in *IEEE International Conference on Robotics and Automation (ICRA)*, Jun. 2015, pp. 5495–5502.
- [16] J. Alonso-Mora, S. Baker, and D. Rus, "Multi-robot formation control and object transport in dynamic environments via constrained optimization," *International Journal of Robotics Research*, vol. 36, no. 9, pp. 1000–1021, 2017.
- [17] G. López-Nicolás, M. Aranda, and Y. Mezouar, "Adaptive multirobot formation planning to enclose and track a target with motion and visibility constraints," *IEEE Transactions on Robotics*, vol. 36, no. 1, pp. 142–156, Feb. 2020.
- [18] J. C. Gower and G. B. Dijkstra, *Procrustes problems*. Oxford University Press, 2004.
- [19] K. Simon and R. Basri, "Elasticity-based matching by minimising the symmetric difference of shapes," *IET Computer Vision*, vol. 12, no. 4, pp. 412–423, 2018.
- [20] J. Das and N. Sarkar, "Autonomous shape control of a deformable object by multiple manipulators," *Journal of Intelligent and Robotic Systems: Theory and Applications*, vol. 62, no. 1, pp. 3–27, 2011.
- [21] M. Roa and R. Suarez, "Grasp quality measures: review and performance," *Autonomous Robots*, vol. 38, pp. 65–88, Jul. 2015.
- [22] B. Siciliano and O. Khatib, Eds., *Springer Handbook of Robotics*. Springer, 2008, chapter 34.
- [23] J.-J. E. Slotine and W. Li, *Applied nonlinear control*. Prentice Hall, Englewood Cliffs NJ, 1991.
- [24] S. Duenser, J. M. Bern, R. Poranne, and S. Coros, "Interactive robotic manipulation of elastic objects," in *IEEE/RSJ International Conference on Intelligent Robots and Systems (IROS)*, 2018, pp. 3476–3481.
- [25] P. Güler, A. Pieropan, M. Ishikawa, and D. Kragic, "Estimating deformability of objects using meshless shape matching," in *IEEE/RSJ International Conference on Intelligent Robots and Systems (IROS)*, 2017, pp. 5941–5948.
- [26] R. Olfati-Saber, J. A. Fax, and R. M. Murray, "Consensus and cooperation in networked multi-agent systems," *Proceedings of the IEEE*, vol. 95, no. 1, pp. 215–233, 2007.
- [27] S. S. Kia, B. Van Scoy, J. Cortes, R. A. Freeman, K. M. Lynch, and S. Martinez, "Tutorial on dynamic average consensus: The problem, its applications, and the algorithms," *IEEE Control Systems Magazine*, vol. 39, no. 3, pp. 40–72, 2019.
- [28] L. J. Latecki, R. Lakamper, and T. Eckhardt, "Shape descriptors for non-rigid shapes with a single closed contour," in *IEEE Conference on Computer Vision and Pattern Recognition (CVPR)*, Jun. 2000, pp. 424–429.